

Phaseformer: Phase-based Attention Mechanism for Underwater Image Restoration and Beyond

MD Raqib Khan¹, Anshul Negi², Ashutosh Kulkarni², Shruti S. Phutke²,
Santosh Kumar Vipparthi², Subrahmanyam Murala¹

¹CVPR Lab, School of Computer Science and Statistics, Trinity College Dublin, Ireland

²CVPR Lab, Indian Institute of Technology Ropar, India

khanmd@tcd.ie

Abstract

Quality degradation is observed in underwater images due to the effects of light refraction and absorption by water, leading to issues like color cast, haziness, and limited visibility. This degradation negatively affects the performance of autonomous underwater vehicles used in marine applications. To address these challenges, we propose a lightweight phase-based transformer network with 1.77M parameters for underwater image restoration (UIR). Our approach focuses on effectively extracting non-contaminated features using a phase-based self-attention mechanism. We also introduce an optimized phase attention block to restore structural information by propagating prominent attentive features from the input. We evaluate our method on both synthetic (UIEB, UFO-120) and real-world (UIEB, U45, UCCS, SQUID) underwater image datasets. Additionally, we demonstrate its effectiveness for low-light image enhancement using the LOL dataset. Through extensive ablation studies and comparative analysis, it is clear that the proposed approach outperforms existing state-of-the-art (SOTA) methods. Code is available at [Phaseformer](#).

Keywords: Phase-attention, Multi-head Attention, Underwater Image Restoration

1. Introduction

Underwater images with higher perceptual quality have a higher significance in marine engineering [45] and aquatic robotics. However, effects like light scattering may degrade the quality of underwater images, including blurriness, reduced brightness, low contrast, and haziness. These degradations significantly affect the performance of underwater applications. To mitigate these challenges, underwater image restoration (UIR) is a feasible solution to enhance the perceptual quality of underwater images, increasing their visibility which potentially leads to improved accuracy in automated underwater applications. Therefore, various researchers proposed algorithms to handle these degradations [7, 12, 23, 40, 45, 72, 77].

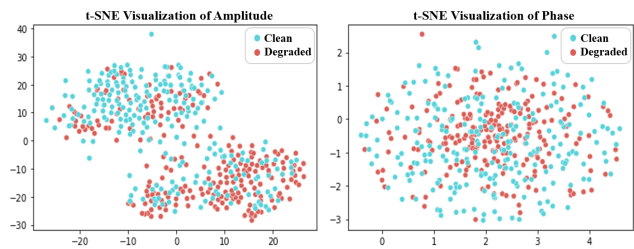


Figure 1. t-SNE visualization of the Amplitude and Phase of clean and degraded images. The separate clusters for clean and degraded amplitude show that there is more effect of degradation on amplitude content as compared to phase content which has overlapping clusters for clean and noisy images.

The prevailing works towards UIE can be classified into three categories. First, the methods following the physical model for estimating the transmission map to generate enhanced images, but it may struggle in complex and dynamic underwater environments [13, 22, 36, 57, 67]. Second, the visual prior-based approaches focus on enhancing visual quality but ignore the physical deterioration process [1, 16, 24, 26, 36]. Last, the deep-learning methods, including transformers, have shown impressive performance in various image restoration tasks, including UIE [18, 55, 60, 64, 65, 74]. Since UIE is a pre-processing task, it is of utmost importance for the UIE architecture to be less computationally complex. Motivated by this, we propose a lightweight architecture for underwater image restoration.

During the underwater image acquisition process, the impact of degradation is greater on the amplitude of image than on the phase [21, 34]. Figure 1 shows the t-SNE visualization of the amplitude and phase of degraded and clean underwater images. This visualization effectively highlights the disparities in the distribution of phase and amplitude between the two sets and offers valuable insights into the impact of degradation on image quality. The separate clusters of amplitude from clean and degraded images show that there is a change in amplitude information of an image

when it is degraded. Whereas, the phase of clean and degraded images have overlapping clusters showing less effect of degradation on it. Since the phase of an image represents structural information [51], it becomes handy to utilize the phase information to enhance the degraded underwater image. With this motivation of phase being less sensitive to degradation, we propose a phase-based self-attention mechanism in the transformer block to achieve efficient color restoration.

The transformer-based U-Net architectures [17] for underwater applications [30, 60] solve the vanishing gradient problem via skip connection between the encoder to the respective decoder. The direct skip connection from the encoder to the decoder may pass even some redundant content. Further, as depth increases the higher wave-length colors get attenuated at a higher rate as well as there may be variations in structural information also. The phase represents the structural information of an image that is less sensitive to degradation (see Figure 1). In light of this, for structural detail propagation from encoder levels to decoder, instead of using direct skip connections, we propose a phase attention block. *To the best of the authors' knowledge, this is the first attempt focused on utilizing the phase-based transformer mechanism for underwater degraded image restoration.*

Also, the proposed network utilizes various losses and the weight of each loss plays an important role to gain optimized results. But manual weight tuning becomes a tedious task. Therefore to solve this issue, we propose an adaptive weight assignment technique that automatically tunes the weights of different losses. Overall, the main contributions of our work are:

- A novel phase-based lightweight transformer (Phase-former) architecture is proposed for underwater image restoration.
- A novel phase-based self-attention mechanism is introduced in the transformer, that operates on the prominent (phase) information of images, enabling it to gather both local and non-local prominent pixel interactions.
- An optimized phase attention block is proposed to forward the attentive structural information from the encoder to the respective decoder for effective restoration.
- An adaptive weight assignment to the loss functions is proposed while training the network for better optimization.

The ablation study is done on different configurations of the proposed approach. We carry out several experiments for demonstrating effectiveness of the proposed method on

both synthetic as well as real-world images for underwater image enhancement. Also, we verify the applicability of the proposed method for low-light enhancement task.

2. Related Work

Initial attempts towards enhancing the underwater images mainly relied on varying the pixel intensities in the red and the blue channels. [17] followed the Rayleigh distribution for obtaining enhanced underwater image by shifting the blue channel portion, while concurrently positioning the red channel in the upper portion. The Jaffe-McGlamery model has served as a foundation for transmission estimation techniques in research [30]. Following this model, [44] optimized the transmission map using a quadtree-based loss function to enhance contrast in the images. [41] estimated the medium transmission via a combination of regression modeling and a global underwater light estimator. For visual result enhancement, [10] proposed a combination of the wavelength-dependent compensation along with the dark channel prior combined with the dark channel prior. [56] proposed an approach involving a generalized dark channel prior, incorporating adaptive color correction for underwater images. However, this method leads to overexposure and incomplete effectiveness in addressing various underwater challenges. [39] extended CNNs with the introduction of the UIEB dataset and Water-Net for UIE. [38] employed synthesized underwater images to train their proposed UWCNN, simulating a realistic underwater environment for image enhancement. [31] introduced a wavelet-corrected transformation for enhancing underwater images. [19] proposed a weakly supervised learning based generative adversarial network, incorporating multiple scaled processing of features. [37] proposed a multi-color processing network for representing a diverse range of color features. For simultaneously enhancing the performance of image enhancement and object detection, [9] introduced dual perceptual enhancement modules for detection, recognizing the need to balance image quality optimization with improved detection outcomes. By analysing the light absorption and blurriness, [57] estimated depth maps for enhancing the visibility in underwater images. Few works [15, 28] utilized conditional adversarial networks (CGAN) for enhancing underwater images. [63] introduced a unified underwater image enhancement and super-resolution approach based on multi-receptive attention. [46] proposed a twin adversarial contrastive learning-based method that further leverages detection-aware training for enhancing the underwater images.

Transformers are widely used in various image restoration tasks. Applications include image dehazing with a hybrid CNN-Transformer [18], efficient image deraining, denoising, and deblurring [74], as well as the “Swin Transformer” [47], for computational efficiency in image denoising and deblurring. Additionally, a U-shaped transformer is

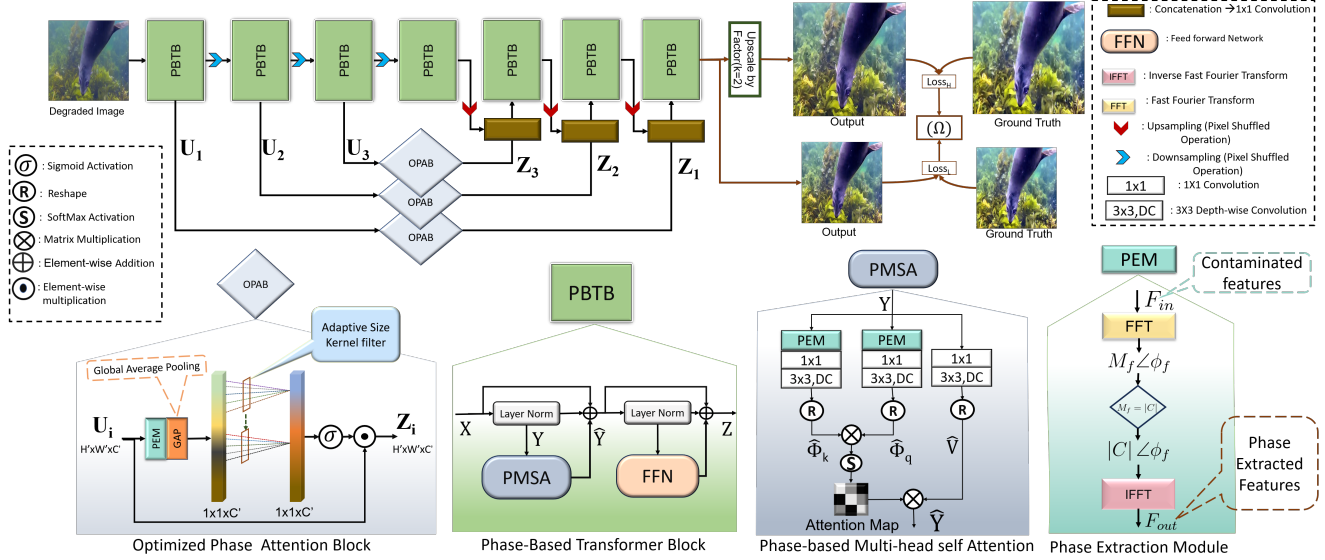


Figure 2. Architectural schematic of the proposed underwater image enhancement network. The network comprises of **Phase-based Transformer Block, Optimized Phase Attention Block, and dynamic weight assignment to the loss functions**. The proposed phase-based transformer block captures local and non-local structural information using less attenuated phase-based queries and keys. Optimized Phase Attention block is proposed for propagating prominent attentive features from the encoder to the respective decoder. The dynamic weight (Ω) assignment is proposed for efficient optimization of the network while training.

used for UIE with feature fusion modules [55].

3. Proposed Method

The existing approaches generally utilize the different color spaces as inputs with separate encoder-decoders to process the original RGB and different color spaces for UIR, which may increase the computational cost of the overall architecture. To mitigate such limitation, here, we propose a lightweight architecture for UIR named "Phase-former: phase-based attention transformer network". For considering the peculiarities of underwater imaging, we propose phase-based self-attention and optimized phase attention. In this paper, we initially illustrate the complete pipeline of our architecture, as shown in Figure 2. Afterward, we provide a detailed overview of the proposed phase-based self-attention and optimized phase attention.

Overall Pipeline: Initially, the input image is passed through a series of proposed phase-based transformer blocks (PBTB) consisting of phase-based self-attention. The features from the initial PBTB are propagated through the proposed optimized phase attention utilized in skip connections. At the final stage, we obtain the outputs with two different resolutions named as actual resolution and $\times 2$ resolution by applying transposed convolution. These multi-resolution outputs are further utilized for loss calculations (see Figure 2). The proposed sub-modules are discussed below:

3.1. Phase-based Transformer Block

Studies show that the phase of an image contains the most relevant information [3, 20, 33, 49, 50, 52, 73], which is sufficient to reconstruct the image completely. Further, it has been observed that the phase of an image is less affected by noise compared to its magnitude [8, 21]. The t-SNE plot depicted in Figure 1 illustrates the comparison between the phase and amplitude of both clean and degraded images. This visualization effectively highlights the disparities in the distribution of phase and amplitude between the two sets and offers valuable insights into the impact of degradation on image quality. As a result, many image processing algorithms place significant emphasis on phase information.

In traditional self-attention mechanism, most of the methods [4, 53, 54, 66, 68] have a time complexity that grows linearly as the input patch size increases. The attention map is generated by computing the dot product of the query and key vectors and applying a softmax function to obtain a probability distribution over the values. Resulting attention map is then used to weigh the value vectors and compute the output of the attention mechanism. However, this approach may not be sufficient for image restoration tasks that require fine-grained spatial relationships. The phase of an image provides valuable spatial information [3, 20, 33, 49, 50, 52, 73]. Incorporating this information into the self-attention mechanism may help to generate more fine-grained and interpretable attention maps that capture the spatial relationships between different parts of

the image. With this motivation, we propose a phase-based self-attention block, shown in Figure 2 that takes structural information through phase features as key and query to generate a more accurate and effective attention map.

In the proposed phase-based transformer block (PBTB), first, the normalized tensor $Y \in \mathbb{R}^{H' \times W' \times C'}$ is fed to the proposed phase-based Multi-head self-attention (PMSA) mechanism (see PBTB in Figure 2). In PMSA, the to generate the structural features for key and query, we proposed a phase extraction module (PEM) (see PMSA in Figure 2). For this, we applied the FFT on input features to extract the phase (ϕ_f) and amplitude (M_f) information. Further, by making $M_f = C$ ($C = 1$) and keeping the phase (ϕ_f) as it is, the IFFT is calculated (see PEM in Figure 2). This operation provides us the prominent phase-only information from the input feature maps which is then fed to the multi-head attention as query (Φ_q) and key (Φ_k).

On these phase-query (Φ_q), phase-key (Φ_k) from PEM, and value (V) from input projection the multi-head attention is applied, which enrich the local context. Subsequently, both query and key projections are reshaped such that their dot-product results in a transposed-attention map (*Attention*) of size $\mathbb{R}^{C' \times C'}$.

$$\hat{\Phi}_q = \varphi_3(\psi_1(PEM(Y))); \quad \hat{\Phi}_k = \varphi_3(\psi_1(PEM(Y))) \quad (1)$$

$$\hat{Y} = \psi_1 \left(\text{Attention} \left(\hat{\Phi}_q, \hat{\Phi}_k, \hat{V} \right) \right) + Y \quad (2)$$

$$\text{Attention} \left(\hat{\Phi}_q, \hat{\Phi}_k, \hat{V} \right) = \hat{V} \cdot \text{Softmax} \left(\frac{\hat{\Phi}_k \cdot \hat{\Phi}_q}{\alpha} \right) \quad (3)$$

where, Y and \hat{Y} are the input and output feature maps of the proposed PMSA. For aggregating pixel-wise cross-channel context, a convolution operator ($\psi_m(\cdot)$) of kernel size ($m \times m$) is used. For channel-wise spatial context, depth-wise convolution operator ($\varphi_m(\cdot)$) of kernel size ($m \times m$) is used, where $m \in (1, 2, 3)$. The network uses bias-free convolution layers. $\hat{\Phi}_q \in \mathbb{R}^{H'W' \times C'}$, $\hat{\Phi}_k \in \mathbb{R}^{C' \times H'W'}$, and $\hat{V} \in \mathbb{R}^{H'W' \times C'}$ matrices are obtained after reshaping tensors from the original size $\mathbb{R}^{H' \times W' \times C'}$. Parameter α can be learned to adjust the dot product of $\hat{\Phi}_q$ and $\hat{\Phi}_k$ before the application of the softmax function. This helps in controlling the magnitude of the dot product. We follow a similar approach as conventional multi-head self-attention (SA) [11], where we split the channels among separate ‘‘heads’’ and learn distinct attention maps in parallel. Further, the \hat{Y} is processed through a feed-forward network (FFN) [75] to get the output of PBTB (Z as shown in PBTB block of Figure 2). Processing the input values with phase based attention helps to restore color information effectively.

3.2. Optimized Phase Attention Block

In general, in order to assist in the reconstruction process skip connections are utilized to forward the encoder

features to the corresponding decoder features [62]. Directly forwarding the features as skip connection may result in some degree of degradation being transferred to the decoder, thereby hindering its ability to efficiently produce an enhanced image. The existing work [55] employed channel-wise multi-scale feature fusion transformer attention to transfer the attentive features from the encoder to the corresponding decoder. However, these attention blocks are computationally expensive and may forward degraded features to the decoder since they are processed in the spatial domain. Moreover, it has been observed that the structural information conveyed through the phase of an image is more resilient to degradation than the amplitude [8, 21]. This property may help with effective image enhancement when only phase information of encoder features is utilized. Therefore, we have introduced a lightweight optimized phase attention block (OPAB), depicted in Figure 2, which generates prominent and attentive features Z_i as:

$$Z_i = U_i \otimes \sigma(\omega_k(\text{GAP}(PEM(U_i)))) \quad (4)$$

where, U_i are the input features of dimension $\frac{H}{2^{i-1}} \times \frac{W}{2^{i-1}} \times 2^{i-1}C$, $i \in (1, 2, 3)$. These, U_i are used to generate phase information by applying a phase extracting module (PEM). Global average pooling operation (GAP) generates the spatially aggregated features with size $1 \times 1 \times 2^{i-1}C$. The ω_k is a 1D convolution operator with adaptive kernel size. In traditional CNNs, the kernel size is fixed and does not change during the training process. However, different encoder features may require different kernel sizes to be effectively captured by the network. This means that some features may be over-smoothed (due to large kernel size) or under-smoothed (due to small kernel size) by the fixed kernel size [2], resulting in loss of important information and hence reduced performance. OPAB addresses this issue by adaptively selecting the kernel size based on the number of input feature channels. It does this by applying a learnable 1D convolution layer to the encoder features, which is then used to weigh the features at each channel. This allows the network to learn which kernel size is best suited to capture the features in each channel of the input. The adaptive kernel size k is determined by:

$$k = \varphi(C') = \left\lfloor \frac{\log_2(C')}{\gamma} + \frac{b}{\gamma} \right\rfloor_{\text{odd}} \quad (5)$$

where, $C' = 2^{i-1}C$ is the number of channels after GAP, $\lfloor t \rfloor_{\text{odd}}$ indicates the nearest odd number of t . In this paper, we set γ and b to 2 and 1 respectively.

3.3. Adaptive Weight Assignment for Training Losses

In deep learning architectures, it is common to train models using multiple loss functions to achieve various objectives simultaneously. However, these loss functions may have different scales or importance levels, which may lead

to difficulty in optimizing the model. To address this issue, we proposed a learnable weight assignment technique, that enables the model to achieve better performance by combining multiple loss functions effectively. It provides a flexible and effective way to balance the trade-offs between different objectives, making it a valuable tool in various applications, such as image restoration.

$$L_T = \Omega_H * L_H + \Omega_L * L_L \quad (6)$$

$$L_R = \Omega_1 * L_C^R + \Omega_2 * L_G^R + \Omega_3 * L_M^R + \Omega_4 * L_P^R \quad (7)$$

L_R represents the total loss with $R \in (L, H)$ (L is low-resolution, H is high-resolution). The adaptive weights ($\Omega_i, i \in \{1, 2, 3, 4\}$) are trainable tensors that are updated during training. These adaptive weights are applied to different loss functions, namely Charbonnier loss (L_C) [6], Gradient loss (L_G) [61], Multi-Scale SSIM (MS-SSIM) loss (L_M) [69], and Perceptual loss (L_P) [32]. At the final epoch, the values of these weights are 0.2741, 0.2222, 0.3357, and 0.1680, respectively. Additionally, empirically determined weights are assigned to the high-resolution loss (L_H) and the low-resolution loss (L_L) as $\Omega_H = 0.4$ and $\Omega_L = 0.6$, respectively. *Comprehensive details regarding the employed loss functions are provided in the supplementary material.*

4. Experimental Discussion

4.1. Datasets

To conduct a comparative analysis, we have considered synthetic underwater UIEB [39], UFO-120 [27] and real-world underwater U45 [42], UCCS [45], and SQUID [5] datasets. The underwater image enhancement benchmark (UIEB) dataset comprises 890 underwater images, featuring various scenes to ensure a wide range of conditions. The training set is composed of randomly selected 800 image pairs, while the remaining 90 images are considered for testing purpose. UFO-120 contains 1500 pairs in training set and a test set of 120 pair samples. U45 comprises 45 real-world images that showcase characteristics such as color casts, low contrast, and the degradation effects resembling haze in underwater scenarios. The SQUID dataset comprises 57 sets of stereo pairs captured at various locations within Israel.

4.2. Training Details

For generating the necessary training images, we applied data augmentation methods, including horizontal and vertical flipping, noise addition, and contrast variation. This led to the creation of 3000/4800 training image pairs and 120/90 testing image pairs from the UFO-120/UIEB datasets, respectively. All input images were resized to

256×256 dimensions. During training, we utilized the ADAM optimizer with initial learning rate of 3×10^{-4} , which was adjusted using the cosine annealing strategy. The implementation of the proposed network was carried out using PyTorch and training was performed on an NVIDIA GeForce RTX 2080 GPU.

4.3. Baselines

For quantitative and qualitative comparison, we have considered UDCP [14], UIBLA [57], RGHS [29], WaterNet [39], FGAN [29], FGAN-UP [29], Deep-Sesr [27], UIECL [43], U-Shape [55], TACL [46], Semi-UIR [25], Spectroformer [35] *etc.* methods of underwater image enhancement.

4.4. Analysis on Synthetic Datasets

We quantitatively compare the proposed method with SOTA techniques using metrics like peak signal-to-noise ratio (PSNR), structural similarity index measure (SSIM), and a non-reference metric of underwater image quality measurement (UIQM). The results for UIEB and UFO-120 datasets can be found in Table 1, and qualitative outcomes are depicted in Figure 3. Our method’s performance aligns competitively with existing approaches.

4.5. Analysis on Real-world Dataset

To assess the effectiveness of the proposed method in real-world scenarios, we present results obtained from the U45 dataset. Our quantitative analysis includes metrics such as UIQM (Underwater Image Quality Measure), UISM (Underwater Image Sharpness Measure), NIQE (Naturalness Image Quality Evaluator), and BRISQUE (Blind/Referenceless Image Spatial Quality Evaluator). The tabulated results can be found in Table 2. Moreover, qualitative outcomes for the U45, UCCS, and SQUID datasets are showcased in Figure 4. The results illustrate that the proposed method significantly improves color balance and visibility in the enhanced images, primarily due to the introduced phase-based mechanisms *Additional quantitative and qualitative outcomes are provided in the supplementary material.*

4.6. Computational Complexity Analysis

Here, we analyze the computational complexity of the proposed method in comparison with the existing SOTA methods, taking into account the number of trainable parameters, floating-point operations (FLOPs), and run time (in seconds per image). As indicated in Table 3, the comparison demonstrates that the proposed method has considerably lower computational complexity than current SOTA methods for UIR.

5. Ablation Study

Following ablation studies are performed on the UIEB [39] dataset for evaluating the effectiveness of each proposed component and the various losses.

Table 1. Quantitative comparison of the proposed method (Ours) with existing SOTA methods for underwater image restoration. (\uparrow) higher is better, **bold** and underline indicate the **best** and second best results.

UIEB								
Method	RGHS	WaterNet	UIECL	U-shape	TACL	Semi-UIR	Spectroformer	Ours
PSNR \uparrow	14.57	19.81	20.37	22.91	23.72	24.59	<u>24.96</u>	25.98
SSIM \uparrow	15.78	0.731	0.864	0.910	0.830	0.901	<u>0.917</u>	0.928
UIQM \uparrow	3.047	3.836	3.544	3.726	3.969	4.598	<u>3.075</u>	<u>4.451</u>
UFO-120								
Method	UDCP	UIBLA	RGHS	FGAN	FGAN-UP	Deep-Sesr	UIECL	Ours
PSNR \uparrow	16.05	20.34	21.03	25.15	24.89	<u>27.15</u>	20.41	30.38
SSIM \uparrow	0.571	0.657	0.739	0.820	0.759	<u>0.840</u>	0.754	0.878
UIQM \uparrow	1.836	1.99	2.271	2.668	2.597	<u>2.749</u>	2.703	2.907

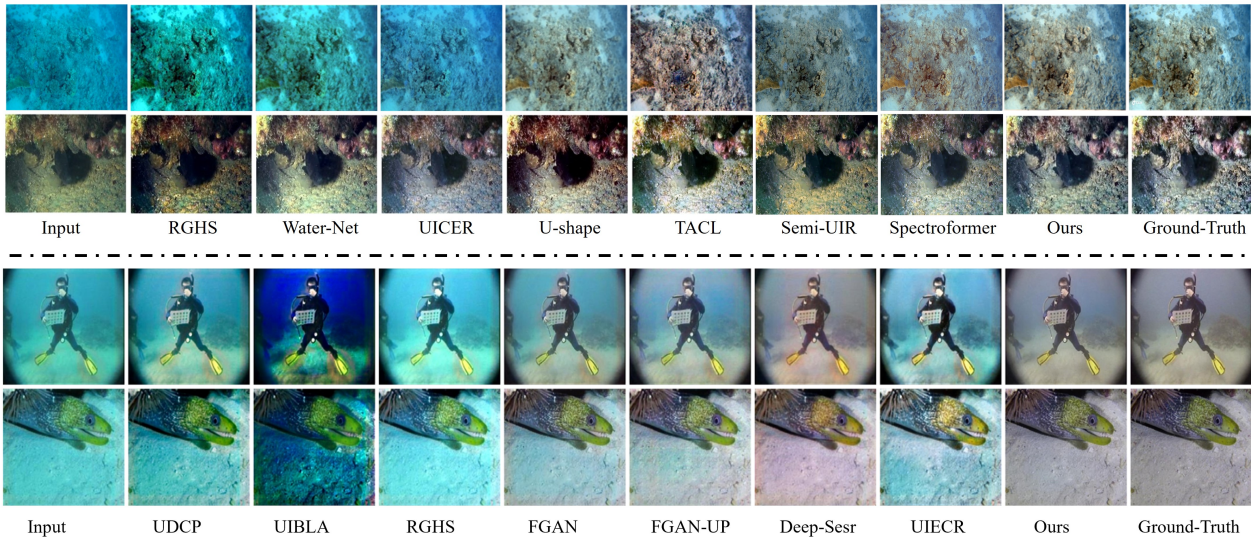


Figure 3. Qualitative comparison of the proposed method (Ours) with existing SOTA methods for underwater image restoration on the synthetic datasets (upper part: UIEB dataset, lower part: UFO-120).

5.1. Effectiveness of the phase-based self-attention in transformer

As the phase of the images is less affected by degradations, the proposed phase-based self-attention mechanism uses phase information to generate an effective attention map for better restoration. To verify this, we tested our hypothesis by conducting experiments with and without phase-based self-attention mechanism. The results, summarized in Table 4, strongly indicate that the phase-based self-attention mechanism contributes to notable improvements

5.2. Effectiveness of the optimized phase attention block in feature propagation

Key features are propagated from encoder levels to the decoder with the incorporation of the proposed optimized phase attention block. We evaluated its influence through experiments by comparing the network’s performance with and without this block. The outcomes shown in Table 4 validate the restored performance achieved when using the

optimized phase attention block.

5.3. Effectiveness of the dynamic weights in optimizing the network losses

Assigning proper weight to each loss plays crucial role, whereas manually assigning the weight to each is a tedious task. Assigning learnable weights for losses may solve this problem. As seen from Table 4, we can verify that the performance with the learnable weights for each loss is better as compared to fixed weights.

5.4. Effectiveness of various loss settings

We also presented the impact of various employed losses on underwater image enhancement, both quantitatively in Table 5 and qualitatively in Figure 5. This comparison shows the effectiveness of utilizing the combination of L_C , L_G , L_M , and L_P .

6. Applications of the Proposed Method

In this section, we explore the practicality of the proposed method for various tasks discussed below.

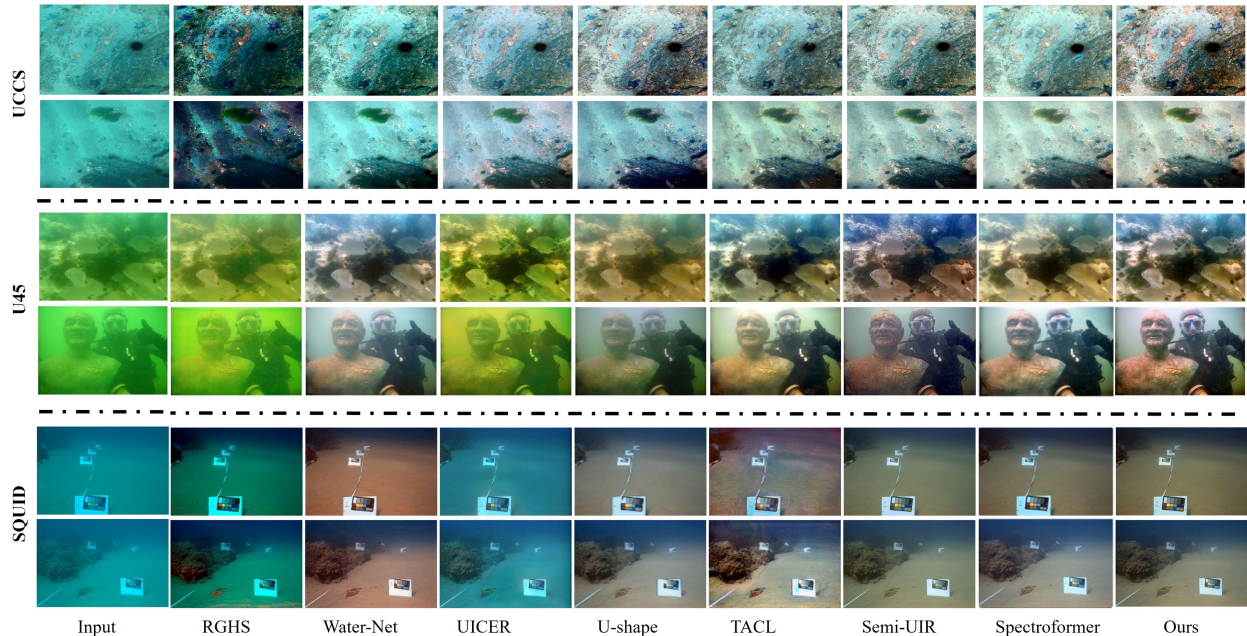


Figure 4. Qualitative comparison of the proposed method (Ours) with existing SOTA methods for underwater image restoration on real-world UCCS, U45, and SQUID datasets.

Table 2. Comparing the proposed method (Ours) with existing state-of-the-art methods on the real-world U45 dataset for underwater image enhancement in terms of quantitative metrics (**bold** and underline indicate the **best** and second best results).

Method	RGHS	WaterNet	UIECL	U-shape	TACL	Semi-UIR	Spectroformer	Ours
UIQM \uparrow	2.506	3.53	3.59	3.63	4.05	<u>4.30</u>	3.243	4.491
UISM \uparrow	5.558	6.187	5.988	5.567	6.698	7.14	7.354	<u>7.532</u>
NIQE \downarrow	3.872	4.596	3.873	4.309	3.992	3.767	3.842	<u>3.811</u>
BRISQUE \downarrow	<u>18.51</u>	21.15	20.61	21.56	20.08	23.02	19.957	18.08
Time(image/sec) \downarrow	0.67	0.370	0.050	0.079	0.059	0.044	<u>0.040</u>	0.034

Table 3. Computation complexity (lower is better) analysis of proposed method with existing methods.

Method	Publication	#Param($\times 10^6$)	FLOPs($\times 10^9$)
WaterNet	TIP-19	24.81	193.7
FGAN	RA-L-20	7.019	10.23
Deep-Sesr	RSS-20	2.40	447.0
U-shape	TIP-23	65.6	66.20
UIECL	TCSVT-22	13.3	31.00
TACL	TIP-22	11.37	56.80
Semi-UIR	CVPR-23	1.67	36.43
Spectroformer	WACV-24	2.40	15.75
Ours	–	<u>1.77</u>	<u>13.0</u>

6.1. Down stream applications

Underwater image restoration as a preprocessing step improves object detection and depth estimation tasks’ performance. Our method shows superior performance on

Table 4. Quantitative results comparison of various network settings and losses optimization. *Note: Self-A: Multihead Self Attention, DW- Dynamic Weights, WDW: without DW, PBSA- phase-based self attention, OA- Optimized Attention (without phase), OPA- Optimized Attention (with phase).*

Self-A	PBSA	DW	OPA	OA	PSNR	SSIM
✓	×	✓	×	×	22.51	0.862
×	✓	✓	×	×	24.24	0.891
×	✓	×	×	✓	24.46	0.901
×	✓	×	✓	×	24.35	0.896
×	✓	✓	✓	×	25.98	0.928

YOLO-v3 [59] for object detection and DPT [58] for depth estimation, as illustrated in Figure 6. The results confirm the applicability of our approach for improving the performance of higher-level computer vision.

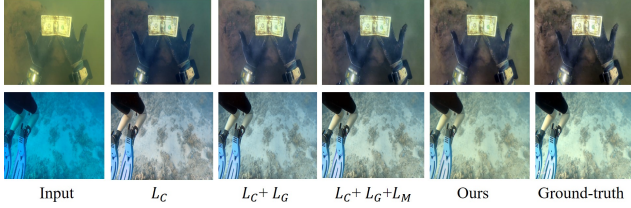


Figure 5. Qualitative comparison of results obtained with various loss settings.

Table 5. Quantitative results comparison of results obtained with various loss settings on UIEB dataset (L_C : Charbonnier loss, L_G : Gradient loss, L_M : Multiscale Structural Similarity Index (MS-SSIM) loss, and L_P : Perceptual loss).

Losses	L_C	L_G	L_M	L_P	PSNR	SSIM
	✓				23.97	0.890
	✓	✓	×	×	24.15	0.907
	✓	✓	✓	×	25.11	0.912
Ours	✓	✓	✓	✓	25.98	0.928

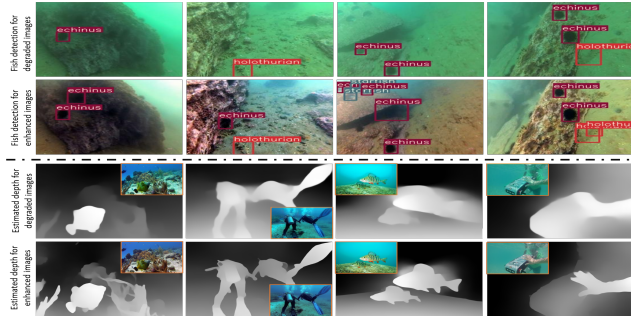


Figure 6. Comparison of degraded images and corresponding enhanced images for fish detection (*upper part*) and depth estimation (*bottom part*) applications.

Table 6. Quantitative results comparison of state-of-the-art (TFFR [48], MIRNetV2 [76]) and the proposed method (Ours) on real world dataset provided in [70].

Methods	NIQE ↓	BRISQUE ↓
TFFR [48]	5.620	29.652
MIRNetV2 [76]	7.513	33.929
Ours	4.535	22.117

6.2. Low-light image enhancement

Low-light image enhancement is another important task that focuses on improving visibility in low-light regions while preserving color consistency and reducing noise. To demonstrate the applicability of our proposed method, we train the network on 970 augmented synthetic image pairs (low-light and ground truth) from [71]. Our method’s performance is showcased through qualitative results depicted in Figure 7, and quantitative evaluations summarized in Table 6, specifically tailored for real-world low-light image enhancement tasks. These results demonstrate the superior-

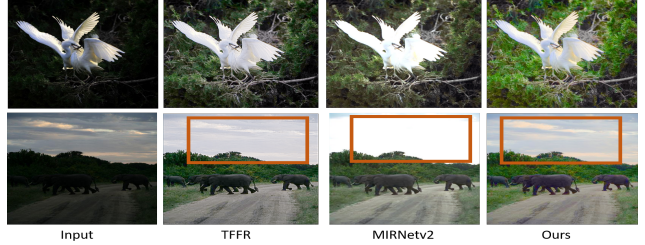


Figure 7. Qualitative comparison of the proposed method (Ours) with existing SOTA methods (TFFR [48], MIRNetV2 [76]) for real-world low light image enhancement.

ity of our proposed method over state-of-the-art techniques in this domain. *Additional, qualitative results are available in the supplementary material.*

7. Failure Case

Analysis of Figure 8 reveals the challenges faced by existing methods in enhancing muddy and blurry underwater images. Despite these difficulties, our approach consistently surpasses current state-of-the-art methods in underwater image enhancement. However, it’s important to note that there remains room for improvement in our outputs, particularly in terms of deblurring. We still need to improve the deblurring aspect of our output, which we are considering for the future scope.

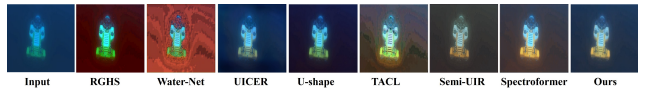


Figure 8. Qualitative results analysis with the proposed (ours) and state-of-the-art methods on the real-world C-60 UIEB dataset for underwater image restoration.

8. Conclusion

This paper introduces a novel lightweight phase-based transformer network for underwater image restoration. The network utilizes a phase-based attention mechanism to extract non-contaminated features effectively, and an optimized phase attention block ensures proper structural reconstruction and prominent feature propagation. Learnable parameters are used to weight the losses during training. Extensive evaluations on synthetic and real-world datasets, along with ablation studies, validate our method’s effectiveness. Its applicability also extends to diverse areas like low-light enhancement, enhanced object detection, and improved depth estimation.

Acknowledgement

This research was supported by MoES (Grant MoES/PAMC/DOM/04/2022 - E-12710), TIHITG202204, and (d-real) Science Foundation Ireland (Grant 18/CRT/6224). The authors thank the CVPR Lab members at Trinity College Dublin and IIT Ropar for their support.

References

- [1] Abdul Ghani, A.S., Mat Isa, N.A.: Underwater image quality enhancement through composition of dual-intensity images and rayleigh-stretching. SpringerPlus **3**(1), 1–14 (2014) [1](#)
- [2] Agrawal, A., Mittal, N.: Using cnn for facial expression recognition: a study of the effects of kernel size and number of filters on accuracy. The Visual Computer **36**(2), 405–412 (2020) [4](#)
- [3] Balaji, Y., Sankaranarayanan, S., Chellappa, R.: Metareg: Towards domain generalization using meta-regularization. In: Bengio, S., Wallach, H., Larochelle, H., Grauman, K., Cesa-Bianchi, N., Garnett, R. (eds.) Advances in Neural Information Processing Systems. vol. 31. Curran Associates, Inc. (2018), <https://proceedings.neurips.cc/paper/2018/file/647bba344396e7c8170902bcf2e15551-Paper.pdf> [3](#)
- [4] Beltagy, I., Peters, M.E., Cohan, A.: Longformer: The long-document transformer. arXiv:2004.05150 (2020) [3](#)
- [5] Berman, D., Treibitz, T., Avidan, S.: Single image dehazing using haze-lines. IEEE transactions on pattern analysis and machine intelligence **42**(3), 720–734 (2018) [5](#)
- [6] Bruhn, A., Weickert, J., Schnörr, C.: Lucas/kanade meets horn/schunck: Combining local and global optic flow methods. International journal of computer vision **61**(3), 211–231 (2005) [5](#)
- [7] Caimi, F.M., Kocak, D.M., Dalglish, F., Watson, J.: Underwater imaging and optics: Recent advances. OCEANS 2008 **2008**, 1–9 (2008) [1](#)
- [8] Chan, T.F., Shen, J.: Image processing and analysis: variational, PDE, wavelet, and stochastic methods. SIAM (2005) [3, 4](#)
- [9] Chen, L., Jiang, Z., Tong, L., Liu, Z., Zhao, A., Zhang, Q., Dong, J., Zhou, H.: Perceptual underwater image enhancement with deep learning and physical priors. IEEE Transactions on Circuits and Systems for Video Technology **31**(8), 3078–3092 (2020) [2](#)
- [10] Chiang, J.Y., Chen, Y.C.: Underwater image enhancement by wavelength compensation and dehazing. IEEE transactions on image processing **21**(4), 1756–1769 (2011) [2](#)
- [11] Dosovitskiy, A., Beyer, L., Kolesnikov, A., Weissenborn, D., Zhai, X., Unterthiner, T., Dehghani, M., Minderer, M., Heigold, G., Gelly, S., et al.: An image is worth 16x16 words: Transformers for image recognition at scale. arXiv preprint arXiv:2010.11929 (2020) [4](#)
- [12] Drap, P.: Underwater photogrammetry for archaeology. Special applications of photogrammetry **114** (2012) [1](#)
- [13] Drews, P., Nascimento, E., Moraes, F., Botelho, S., Campos, M.: Transmission estimation in underwater single images. In: Proceedings of the IEEE international conference on computer vision workshops. pp. 825–830 (2013) [1](#)
- [14] Drews, P.L., Nascimento, E.R., Botelho, S.S., Campos, M.F.M.: Underwater depth estimation and image restoration based on single images. IEEE computer graphics and applications **36**(2), 24–35 (2016) [5](#)
- [15] Fabbri, C., Islam, M.J., Sattar, J.: Enhancing underwater imagery using generative adversarial networks. In: 2018 IEEE International Conference on Robotics and Automation (ICRA). pp. 7159–7165. IEEE (2018) [2](#)
- [16] Fu, X., Zhuang, P., Huang, Y., Liao, Y., Zhang, X.P., Ding, X.: A retinex-based enhancing approach for single underwater image. In: 2014 IEEE international conference on image processing (ICIP). pp. 4572–4576. IEEE (2014) [1](#)
- [17] Ghani, A.S.A., Isa, N.A.M.: Underwater image quality enhancement through integrated color model with rayleigh distribution. Applied soft computing **27**, 219–230 (2015) [2](#)
- [18] Guo, C.L., Yan, Q., Anwar, S., Cong, R., Ren, W., Li, C.: Image dehazing transformer with transmission-aware 3d position embedding. In: Proceedings of the IEEE/CVF Conference on Computer Vision and Pattern Recognition. pp. 5812–5820 (2022) [1, 2](#)
- [19] Guo, Y., Li, H., Zhuang, P.: Underwater image enhancement using a multiscale dense generative adversarial network. IEEE Journal of Oceanic Engineering **45**(3), 862–870 (2019) [2](#)
- [20] Hansen, B.C., Hess, R.F.: Structural sparseness and spatial phase alignment in natural scenes. JOSA A **24**(7), 1873–1885 (2007) [3](#)
- [21] Haykin, S.: Communication systems. John Wiley & Sons (2008) [1, 3, 4](#)

- [22] He, K., Sun, J., Tang, X.: Single image haze removal using dark channel prior. *IEEE transactions on pattern analysis and machine intelligence* **33**(12), 2341–2353 (2010) [1](#)
- [23] Henderson, J., Pizarro, O., Johnson-Roberson, M., Mahon, I.: Mapping submerged archaeological sites using stereo-vision photogrammetry. *International Journal of Nautical Archaeology* **42**(2), 243–256 (2013) [1](#)
- [24] Huang, D., Wang, Y., Song, W., Sequeira, J., Mavromatis, S.: Shallow-water image enhancement using relative global histogram stretching based on adaptive parameter acquisition. In: *MultiMedia Modeling: 24th International Conference, MMM 2018, Bangkok, Thailand, February 5-7, 2018, Proceedings, Part I* 24. pp. 453–465. Springer (2018) [1](#)
- [25] Huang, S., Wang, K., Liu, H., Chen, J., Li, Y.: Contrastive semi-supervised learning for underwater image restoration via reliable bank. In: *Proceedings of the IEEE/CVF Conference on Computer Vision and Pattern Recognition*. pp. 18145–18155 (2023) [5](#)
- [26] Iqbal, K., Odetayo, M., James, A., Salam, R.A., Talib, A.Z.H.: Enhancing the low quality images using unsupervised colour correction method. In: *2010 IEEE International Conference on Systems, Man and Cybernetics*. pp. 1703–1709. IEEE (2010) [1](#)
- [27] Islam, M.J., Luo, P., Sattar, J.: Simultaneous enhancement and super-resolution of underwater imagery for improved visual perception. *arXiv preprint arXiv:2002.01155* (2020) [5](#)
- [28] Islam, M.J., Xia, Y., Sattar, J.: Fast underwater image enhancement for improved visual perception. *IEEE Robotics and Automation Letters (RA-L)* **5**(2), 3227–3234 (2020) [2](#)
- [29] Islam, M.J., Xia, Y., Sattar, J.: Fast underwater image enhancement for improved visual perception. *IEEE Robotics and Automation Letters* **5**(2), 3227–3234 (2020) [5](#)
- [30] Jaffe, J.S.: Computer modeling and the design of optimal underwater imaging systems. *IEEE Journal of Oceanic Engineering* **15**(2), 101–111 (1990) [2](#)
- [31] Jamadandi, A., Mudenagudi, U.: Exemplar-based underwater image enhancement augmented by wavelet corrected transforms. In: *Proceedings of the IEEE/CVF Conference on Computer Vision and Pattern Recognition Workshops*. pp. 11–17 (2019) [2](#)
- [32] Johnson, J., Alahi, A., Fei-Fei, L.: Perceptual losses for real-time style transfer and super-resolution. In: *Computer Vision—ECCV 2016: 14th European Conference, Amsterdam, The Netherlands, October 11-14, 2016, Proceedings, Part II* 14. pp. 694–711. Springer (2016) [5](#)
- [33] Juvells, I., Vallmitjana, S., Carnicer, A., Campos, J.: The role of amplitude and phase of the fourier transform in the digital image processing. *American Journal of Physics* **59**(8), 744–748 (1991) [3](#)
- [34] Khan, M.R., Kulkarni, A., Phutke, S.S., Murala, S.: Underwater image enhancement with phase transfer and attention. In: *2023 International Joint Conference on Neural Networks (IJCNN)*. pp. 1–8. IEEE (2023) [1](#)
- [35] Khan, R., Mishra, P., Mehta, N., Phutke, S.S., Vipparthi, S.K., Nandi, S., Murala, S.: Spectroformer: Multi-domain query cascaded transformer network for underwater image enhancement. In: *Proceedings of the IEEE/CVF Winter Conference on Applications of Computer Vision*. pp. 1454–1463 (2024) [5](#)
- [36] Li, C.Y., Guo, J.C., Cong, R.M., Pang, Y.W., Wang, B.: Underwater image enhancement by dehazing with minimum information loss and histogram distribution prior. *IEEE Transactions on Image Processing* **25**(12), 5664–5677 (2016) [1](#)
- [37] Li, C., Anwar, S., Hou, J., Cong, R., Guo, C., Ren, W.: Underwater image enhancement via medium transmission-guided multi-color space embedding. *IEEE Transactions on Image Processing* **30**, 4985–5000 (2021) [2](#)
- [38] Li, C., Anwar, S., Porikli, F.: Underwater scene prior inspired deep underwater image and video enhancement. *Pattern Recognition* **98**, 107038 (2020) [2](#)
- [39] Li, C., Guo, C., Ren, W., Cong, R., Hou, J., Kwong, S., Tao, D.: An underwater image enhancement benchmark dataset and beyond. *IEEE Transactions on Image Processing* **29**, 4376–4389 (2019) [2](#), [5](#)
- [40] Li, C., Guo, J., Guo, C.: Emerging from water: Underwater image color correction based on weakly supervised color transfer. *IEEE Signal processing letters* **25**(3), 323–327 (2018) [1](#)
- [41] Li, C., Guo, J., Guo, C., Cong, R., Gong, J.: A hybrid method for underwater image correction. *Pattern Recognition Letters* **94**, 62–67 (2017) [2](#)
- [42] Li, H., Li, J., Wang, W.: A fusion adversarial underwater image enhancement network with a public test dataset. *arXiv preprint arXiv:1906.06819* (2019) [5](#)

- [43] Li, K., Wu, L., Qi, Q., Liu, W., Gao, X., Zhou, L., Song, D.: Beyond single reference for training: underwater image enhancement via comparative learning. *IEEE Transactions on Circuits and Systems for Video Technology* (2022) **5**
- [44] Liu, H., Chau, L.P.: Underwater image restoration based on contrast enhancement. In: *2016 IEEE International Conference on Digital Signal Processing (DSP)*. pp. 584–588. IEEE (2016) **2**
- [45] Liu, R., Fan, X., Zhu, M., Hou, M., Luo, Z.: Real-world underwater enhancement: Challenges, benchmarks, and solutions under natural light. *IEEE Transactions on Circuits and Systems for Video Technology* **30**(12), 4861–4875 (2020) **1, 5**
- [46] Liu, R., Jiang, Z., Yang, S., Fan, X.: Twin adversarial contrastive learning for underwater image enhancement and beyond. *IEEE Transactions on Image Processing* **31**, 4922–4936 (2022) **2, 5**
- [47] Liu, Z., Lin, Y., Cao, Y., Hu, H., Wei, Y., Zhang, Z., Lin, S., Guo, B.: Swin transformer: Hierarchical vision transformer using shifted windows. In: *Proceedings of the IEEE/CVF International Conference on Computer Vision*. pp. 10012–10022 (2021) **2**
- [48] Ma, L., Ma, T., Liu, R., Fan, X., Luo, Z.: Toward fast, flexible, and robust low-light image enhancement. In: *Proceedings of the IEEE/CVF Conference on Computer Vision and Pattern Recognition (CVPR)*. pp. 5637–5646 (June 2022) **8**
- [49] Oppenheim, A., Lim, J., Kopec, G., Pohlig, S.: Phase in speech and pictures. In: *ICASSP'79. IEEE International Conference on Acoustics, Speech, and Signal Processing*. vol. 4, pp. 632–637. IEEE (1979) **3**
- [50] Oppenheim, A.V., Lim, J.S.: The importance of phase in signals. *Proceedings of the IEEE* **69**(5), 529–541 (1981) **3**
- [51] Oppenheim, A., Lim, J.: The importance of phase in signals. *Proceedings of the IEEE* **69**(5), 529–541 (1981). <https://doi.org/10.1109/PROC.1981.12022> **2**
- [52] Park, S., Park, J., Shin, S.J., Moon, I.C.: Adversarial dropout for supervised and semi-supervised learning. In: *Proceedings of the AAAI conference on artificial intelligence*. vol. 32 (2018) **3**
- [53] Parmar, N.J., Vaswani, A., Uszkoreit, J., Kaiser, L., Shazeer, N., Ku, A., Tran, D.: Image transformer. In: *International Conference on Machine Learning (ICML)* (2018), <http://proceedings.mlr.press/v80/parmar18a.html> **3**
- [54] Peng, H., Pappas, N., Yogatama, D., Schwartz, R., Smith, N.A., Kong, L.: Random feature attention. *CoRR* **abs/2103.02143** (2021), <https://arxiv.org/abs/2103.02143> **3**
- [55] Peng, L., Zhu, C., Bian, L.: U-shape transformer for underwater image enhancement. In: *Computer Vision–ECCV 2022 Workshops: Tel Aviv, Israel, October 23–27, 2022, Proceedings, Part II*. pp. 290–307. Springer (2023) **1, 3, 4, 5**
- [56] Peng, Y.T., Cao, K., Cosman, P.C.: Generalization of the dark channel prior for single image restoration. *IEEE Transactions on Image Processing* **27**(6), 2856–2868 (2018) **2**
- [57] Peng, Y.T., Cosman, P.C.: Underwater image restoration based on image blurriness and light absorption. *IEEE transactions on image processing* **26**(4), 1579–1594 (2017) **1, 2, 5**
- [58] Ranftl, R., Bochkovskiy, A., Koltun, V.: Vision transformers for dense prediction. *ArXiv preprint* (2021) **7**
- [59] Redmon, J., Farhadi, A.: Yolov3: An incremental improvement. *arXiv preprint arXiv:1804.02767* (2018) **7**
- [60] Ren, T., Xu, H., Jiang, G., Yu, M., Luo, T.: Reinforced swin-convs transformer for underwater image enhancement. *arXiv preprint arXiv:2205.00434* (2022) **1, 2**
- [61] Ribeiro, J., Elsayed, E.: A case study on process optimization using the gradient loss function. *International Journal of Production Research* **33**(12), 3233–3248 (1995) **5**
- [62] Ronneberger, O., Fischer, P., Brox, T.: U-net: Convolutional networks for biomedical image segmentation. In: *Medical Image Computing and Computer-Assisted Intervention–MICCAI 2015: 18th International Conference, Munich, Germany, October 5–9, 2015, Proceedings, Part III* 18. pp. 234–241. Springer (2015) **4**
- [63] Sharma, P.K., Bisht, I., Sur, A.: Wavelength-based attributed deep neural network for underwater image restoration (2021) **2**
- [64] Tsai, F.J., Peng, Y.T., Lin, Y.Y., Tsai, C.C., Lin, C.W.: Stripformer: Strip transformer for fast image deblurring. In: *Computer Vision–ECCV 2022: 17th European Conference, Tel Aviv, Israel, October 23–27, 2022, Proceedings, Part XIX*. pp. 146–162. Springer (2022) **1**

- [65] Valanarasu, J.M.J., Yasarla, R., Patel, V.M.: Transweather: Transformer-based restoration of images degraded by adverse weather conditions. In: Proceedings of the IEEE/CVF Conference on Computer Vision and Pattern Recognition. pp. 2353–2363 (2022) [1](#)
- [66] Wang, S., Li, B., Khabsa, M., Fang, H., Ma, H.: Linformer: Self-attention with linear complexity (2020), <http://arxiv.org/abs/2006.04768>, cite arxiv:2006.04768 [3](#)
- [67] Wang, Y., Liu, H., Chau, L.P.: Single underwater image restoration using adaptive attenuation-curve prior. IEEE Transactions on Circuits and Systems I: Regular Papers **65**(3), 992–1002 (2017) [1](#)
- [68] Wang, Z., Ng, P., Ma, X., Nallapati, R., Xiang, B.: Multi-passage bert: A globally normalized bert model for open-domain question answering. In: EMNLP 2019 (2019), <https://www.amazon.science/publications/multi-passage-bert-a-globally-normalized-bert-model-for-open-domain-question-answering> [3](#)
- [69] Wang, Z., Simoncelli, E.P., Bovik, A.C.: Multiscale structural similarity for image quality assessment. In: The Thirty-Seventh Asilomar Conference on Signals, Systems & Computers, 2003. vol. 2, pp. 1398–1402. Ieee (2003) [5](#)
- [70] Wei, C., Wang, W., Yang, W., Liu, J.: Deep retinex decomposition for low-light enhancement. In: British Machine Vision Conference (2018) [8](#)
- [71] Wei, C., Wang, W., Yang, W., Liu, J.: Deep retinex decomposition for low-light enhancement. arXiv preprint arXiv:1808.04560 (2018) [8](#)
- [72] Williams, D.P.: On optimal auv track-spacing for underwater mine detection. In: 2010 IEEE International Conference on Robotics and Automation. pp. 4755–4762. IEEE (2010) [1](#)
- [73] Xu, Q., Zhang, R., Zhang, Y., Wang, Y., Tian, Q.: A fourier-based framework for domain generalization. In: Proceedings of the IEEE/CVF Conference on Computer Vision and Pattern Recognition (CVPR). pp. 14383–14392 (June 2021) [3](#)
- [74] Zamir, S.W., Arora, A., Khan, S., Hayat, M., Khan, F.S., Yang, M.H.: Restormer: Efficient transformer for high-resolution image restoration. In: CVPR (2022) [1](#), [2](#)
- [75] Zamir, S.W., Arora, A., Khan, S., Hayat, M., Khan, F.S., Yang, M.H.: Restormer: Efficient transformer for high-resolution image restoration. In: Proceedings of the IEEE/CVF Conference on Computer Vision and Pattern Recognition. pp. 5728–5739 (2022) [4](#)
- [76] Zamir, S.W., Arora, A., Khan, S., Hayat, M., Khan, F.S., Yang, M.H., Shao, L.: Learning enriched features for fast image restoration and enhancement. IEEE Transactions on Pattern Analysis and Machine Intelligence (TPAMI) (2022) [8](#)
- [77] Zhang, W., Wang, Y., Li, C.: Underwater image enhancement by attenuated color channel correction and detail preserved contrast enhancement. IEEE Journal of Oceanic Engineering **47**(3), 718–735 (2022) [1](#)